Monthly Notices of the ROYAL ASTRONOMICAL SOCIETY

MNRAS **545,** 1–8 (2026) https://doi.org/10.1093/mnras/staf2160
Advance Access publication 2025 December 8

History of UHECR production in Centaurus A

Cainã de Oliveira ★ and Vitor de Souza
Instituto de Física de São Carlos, Universidade de São Paulo, Av. Trabalhador São-carlense 400, São Carlos, Brasil

Accepted 2025 November 28. Received 2025 November 19; in original form 2025 July 31

ABSTRACT

The origin of ultra-high-energy cosmic rays (UHECRs) remains a puzzle more than 50 yr after their discovery. Yet, the well-established excess of events toward the radio galaxy Centaurus A (Cen A) raises the possibility that it is the first identifiable UHECR source. Although Cen A has been considered as a UHECR source, its present jet activity seems unable to explain the most energetic events. Recently, the lobes of radio galaxies have been proposed as potential reservoirs of UHECRs, from which particles accelerated in previous episodes of higher activity slowly escape. In this work, we investigated whether the past activity episodes of Cen A could be related to the UHECR excess observed in the *Centaurus region*. By modelling the UHECR propagation in the Giant Lobes of Cen A, we tested the reservoir hypothesis and its connection with the activity history of Cen A. By analysing the energies of the events and the overall mass composition of UHECRs, we find that activity within the last ~ 30 Myr is required to explain the excess. This period aligns closely with the time-scale where the transition regions and the Giant Lobes must be energized, as revealed by radio and γ ray observations.

Key words: acceleration of particles – astroparticle physics – diffusion – magnetic fields – quasars: individual: Centaurus A.

1 INTRODUCTION

The origin of ultra-high-energy cosmic rays (UHECR) has remained unknown for more than half a century (J. Linsley 1963). Charged particles are deflected by the Galactic and extragalactic magnetic fields, making it difficult to trace them back to their sources. Deflections are smaller for higher-energy particles from nearby sources. Moreover, the most energetic particles likely originate within ∼100 Mpc, as energy losses from interactions with the cosmic microwave and extragalactic background light limit their travel distance (K. Greisen 1966; G. T. Zatsepin & V. A. Kuzmin 1966; R. G. Lang et al. 2020). This supports the prospect of conducting UHECR astronomy focused on nearby sources (J. W. Cronin 1999).

The possibility of UHECR acceleration in radio galaxies and particularly Centaurus A (Cen A) has been discussed over the years (e.g. G. E. Romero et al. 1996; J. H. Matthews et al. 2018a; F. M. Rieger 2022; S. Mollerach & E. Roulet 2024). Cen A is the nearby AGN, at 3.8 ± 0.1 Mpc (G. L. Harris, M. Rejkuba & W. E. Harris 2010), making it an ideal target for UHECR astronomy. In addition, its proximity, angular size ($\sim 9^\circ$), and relative orientation enable high-quality multiwavelength observations, revealing its history and spatial structures (F. Israel 1998; J. H. Croston et al. 2009; Sun, Xiao-na et al. 2016; The H.E.S.S. Collaboration 2020; B. McKinley et al. 2022).

The hypothesis of Cen A as a UHECR source was reinforced with the detection of an excess of UHECR events pointing only 2° away from it, the *Centaurus excess* (A. Abdul Halim et al. 2023a). Cen A is the obvious candidate for the source (R.-Y. Liu et al. 2012; C. a. Oliveira & V. Souza 2022, 2023), despite alternative scenarios also being discussed (C. a. Oliveira & V. Souza 2023; H.-N. He et al. 2024). Detailed analyses (e.g. J. H. Matthews et al. 2018a, b) suggest that the current activity of Cen A satisfies the power constraints necessary to accelerate the more energetic UHECRs only for highly ideal scenarios. Acceleration to ultra-high energies in the lobes is also subject to controversy (M. J. Hardcastle et al. 2009; R.-Y. Liu et al. 2012). However, a powerful past activity cannot be ruled out, and in this case, the radio lobes would be UHECR reservoirs (J. H. Matthews et al. 2018a, b).

In this work, we identify the time window during which UHECRs accelerated on the inner structure of Cen A remain confined within the lobe for long enough to be detected. This is the first time (to our knowledge) that the history of an astrophysical object, obtained from actual observations, is potentially connected with the acceleration of UHECRs. We investigate the previously proposed reservoir hypothesis through a detailed study of UHECR propagation within the Giant Lobes of Cen A. The analysis enables us to constrain the past activity likely to be responsible for the currently observed events. In Section 2, we identify the time window during which UHECRs remain confined in the lobes. In Section 3, we demonstrate that the energization time-scale of the Giant Lobes of Cen A is consistent with the production of UHECRs that contribute to the *Centaurus excess* observed by the Pierre Auger Observatory, taking into account both composition and energetic requirements. The main results and implications are summarized in Section 4.

2 TIME CONSTRAINTS OF ACCELERATION OF PARTICLES IN CEN A

In this section, we calculate the residence time of UHECRs in Cen A's Outer lobes. This time is compared to the history of events and

★ E-mail: olivcaina@gmail.com

the age of structures in Cen A, as well as the data measured by the Pierre Auger Observatory.

The radio structure of Cen A reveals three extended regions around the central galaxy, known as Giant/Outer lobes, Northern Middle Lobe, and Inner Lobes (F. Israel 1998). Giant Lobes (Northern and Southern) have a size larger than 480 kpc and a dynamic age of ~ 1.6 Gyr, probably resulting from past activity events (B. McKinley et al. 2022). The jet of Cen A is currently active, being responsible for the formation of the Inner Lobes. Each Inner Lobe is ~ 5 kpc long and $\sim$ 1–2 Myr old (S. G. Neff, J. A. Eilek & F. N. Owen 2015a). The Northern Middle Lobe (referred to as Middle Lobe in this study) is the northern transition region connecting the Inner and Giant Lobes. It is characterized by aligned radio and X-ray knots and filaments resembling a large-scale jet. Its origin has been proposed as the interaction of a broad, large-scale outflow (from the AGN or starburst activity) boosted by an AGN jet outburst, with cold and warm gas clouds, producing a region of turbulence and inducing star formation (S. G. Neff, J. A. Eilek & F. N. Owen 2015b; B. McKinley et al. 2022). Ongoing starburst activity is also observed in Cen A. It has an age $\gtrsim 50$ Myr, with recent star formation occurring over the past 2–50 Myr (S. G. Neff et al. 2015b). These time-scales and spatial extents will be compared with the expected escape of UHECR from the lobes.

The estimated power of the current jet activity, $\sim 2 \times 10^{43}$ erg s^{-1} (S. G. Neff et al. 2015a), is sufficient to produce the most energetic UHECRs only under ideal scenarios (J. H. Matthews et al. 2018a, b). However, Cen A shows evidence for episodes of higher activity in the past, leading to the hypothesis that its lobes act as UHECR reservoirs (J. H. Matthews et al. 2018a, b). Recent observations from B. McKinley et al. (2022) revealed a clear gap between the Inner Lobe and the first radio knot in the Middle Lobe, which disfavours the existence of a currently operating large-scale jet. Nevertheless, a previous jet likely carved a cocoon in the medium, channelling the current outflow (B. McKinley et al. 2022). As argued by S. G. Neff et al. (2015a) and S. G. Neff et al. (2015b), Cen A's jet likely undergoes reactivation cycles every few Myr. This supports the idea of intermittent AGN activity, with potentially intensive phases driven by cold accretion modes. Variability near the jet base has also been reported [see B. McKinley et al. (2022) and references therein].

To estimate a time-scale of higher activity, potentially relevant for UHECR acceleration, we examine the lifetimes of structures in the Outer and Middle Lobes. Radio and γ-ray emissions observed in the Outer Lobes limit the energy supply to no longer than ~ 30 Myr ago (M. J. Hardcastle et al. 2009; J. A. Eilek 2014). Energy flows through the transition regions is necessary to energize the Giant Lobes. The presence of short-lived structures in the Middle Lobe requires re-energization within $\lesssim 10$ Myr (S. G. Neff et al. 2015a, b). We will refer to the period $\sim$ 10–30 Myr as the re-energization phase.

To connect the history of activity in Cen A with the UHECR signal currently measured at Earth, it is necessary to account for the time delays to which UHECRs are subject. We assume that any of the internal structures in Cen A (jet, Inner Lobes, or transition regions) could accelerate UHECRs. After being injected from the acceleration site, the time necessary to detect the particles is the sum of the time to escape the source ($\tau_{\rm esc}$) and time delays from the extragalactic and Galactic propagation ($\delta t_{\rm prop}$). Given the age and size of the Giant Lobes, UHECRs possibly accelerated in any of the internal structures will need to cross them before escaping to the interstellar medium. In the case where acceleration occurs in the Giant Lobes, the constraints derived below can be seen as upper limits, since particles do not necessarily need to cross the entire lobe extension to escape.

Radio galaxy lobes are filamentary and magnetized environments (S. O'Sullivan, B. Reville & A. M. Taylor 2009; S. Wykes et al. 2014). In these circumstances, the escape time can be estimated from a combination of microscopic propagation regimes and advection of particles in the ambient plasma. During the propagation within the Giant Lobes, energy losses could modulate the energy spectrum. However, as shown in Appendix A, energy losses inside the Giant Lobes can be neglected for the energy range we are considering.

Microscopic propagation involves the transition between rectilinear and diffusive regimes. We model the lobes of Cen A as a turbulent, approximately spherical medium. As shown by R. Aloisio, V. Berezinsky & A. Gazizov (2009), for isotropic turbulence and injection, these regimes can be fully described by the generalized propagator

$$P_J(r,t,E) = \frac{\Theta(ct-r)}{4\pi(ct)^3}\frac{\alpha(t,E)}{K_1(\alpha(t,E))}\frac{e^{-\alpha/\sqrt{1-(r/ct)^2}}}{[1-(r/ct)^2]^2}, \quad (1)$$

where K_1 is the Bessel function and $\alpha(t,E) = c^2 t/2D(E)$, in the absence of energy losses.

For rectilinear propagation, particles take $\tau_{\rm rect} = L/c$ to escape a region of size L. The same distance is travelled in a time-scale $\tau_{\rm dif} = L^2/6D(E)$ in the diffusive regime. Considering equation (1), a general time-scale to cross L can be obtained by writing

$$\tau_{\rm esc}(E) = \frac{L^2}{\langle r^2\rangle(L/c,E)}\frac{L}{c}, \quad (2)$$

where $\langle r^2\rangle(t,E) = \int r^2 P_J(r,t,E)d^3r$, and we use the definition $D = \langle r^2\rangle/6t$. Along this work, we adopt the diffusion coefficient found by D. Harari, S. Mollerach & E. Roulet (2014)

$$D(E) = \frac{c}{3}\ell_{\rm c}\left[4\left(\frac{E}{E_{\rm c}}\right)^2 + 0.9\frac{E}{E_{\rm c}} + 0.23\left(\frac{E}{E_{\rm c}}\right)^{1/3}\right] \quad (3)$$

where $E_c = 0.9Z\,(B_{\rm rms}/\mu{\rm G})\,(\ell_c/{\rm kpc})$ EeV, $B_{\rm rms}$ is the root mean square of the magnetic field intensity, and $\ell_{\rm c}$ its coherence length. We assume a Kolmogorov spectrum for the magnetic field turbulence. Radio and γ-ray measurements from the Giant Lobes indicate $B_{\rm rms} \approx 1$ μG (M. J. Hardcastle et al. 2009; I. I. Stefan et al. 2013; J. A. Eilek 2014; Sun, Xiao-na et al. 2016). Observations of radio filaments in the southern Giant Lobe suggest the scale $\ell_{\rm max} \sim 50$ kpc (J. A. Eilek 2014; S. Wykes, M. J. Hardcastle & J. H. Croston 2015), implying $\ell_c \sim 10$ kpc for a Kolmogorov turbulence (D. Harari et al. 2002).

Advection can play an important role in the escape from lobes. As discussed by J. H. Matthews & A. M. Taylor (2021), a reliable estimation for the advection time-scale $\tau_{\rm adv} = L/v_{\rm adv}$ is hard to obtain. For Cen A, a large-scale outflow with speed of ~ 1100 km s^{-1} is measured (B. McKinley et al. 2022). Despite the outflow should thermalize at a radius ~ 75 kpc (B. McKinley et al. 2022), we take the pragmatic approach of using its speed to estimate the advection time-scale.

The exact value of L depends on the exact structure and time at which the acceleration happened. Based on the size of the Giant Lobes and the spherical approximation, we consider $L \sim 200$ kpc.

Fig. 1 shows the time necessary for UHECRs to escape the Giant Lobes of Cen A for different UHECR species. UHECRs of higher energies follow rectilinear trajectories, and escape the lobes after ~ 0.6 Myr. However, diffusion starts to be important for

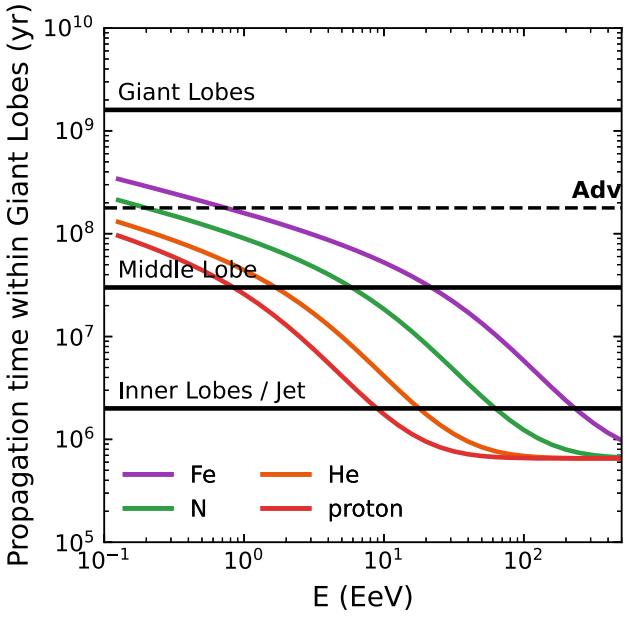

Figure 1. Time necessary for UHECRs to escape the Giant Lobes of Cen A for different UHECR species. The age and time-scales for different structures in Cen A (continuous black lines) and the advection time-scale inside the lobes (black dashed line indicated by Adv) are also shown. The Middle Lobe time-scale is taken as 30 Myr.

lower energies ($\lesssim 10$ EeV for protons and $\lesssim 100$ EeV for nitrogen), causing a significant delay in the escape time. In general, advection is only important below ~ 1 EeV and can be neglected for our purposes. Considering the age of the current activity, only UHECRs with energies above $\sim$ 10–100 EeV have enough time to escape the Giant Lobes. For particles possibly accelerated during the Middle/Giant-Lobes re-energization time-scale, only protons with energies $\gtrsim 1$ EeV and iron with energies $\gtrsim 20$ EeV would have escaped.

After escaping the Giant Lobes, particles will propagate through the extragalactic environment before hitting Earth. Extragalactic magnetic fields delay the arrival time of UHECRs compared to a rectilinear propagation. S. Mollerach & E. Roulet (2024) estimate an increase $\delta t_{\rm prop} \sim \theta^2_{\rm rms} d/6c$. To estimate $\delta t_{\rm prop}$ for UHECRs within the *Centaurus excess*, we adopt $d = 3.8$ Mpc (G. L. Harris et al. 2010) and the scattering angle as the excess radius $\theta \sim 27^\circ$ (A. Abdul Halim et al. 2025b). This results in a time delay $\delta t_{\rm prop} \sim 0.5$ Myr for UHECRs populating the *excess*. Despite that, larger time delays were proposed by R. Mbarek & D. Caprioli (2025), depending on particles' rigidity and the coherence length of the extragalactic magnetic field. In this case, we expect larger deflection angles.

The time-scales obtained proved that UHECRs injected by Cen A are likely to remain imprisoned inside the Giant Lobes. The residence time depends on the energy and charge of the particles, varying from ~ 0.6 Myr for particles performing a rectilinear propagation to ~ 100 Myr for less energetic diffusing particles. These time-scales likely dominate the time delay caused by the extragalactic propagation (~ 0.5 Myr) in the limit of small scattering. Only light (proton, helium) particles with energies above ~ 10 EeV accelerated from the current activity of Cen A had time to escape from the Giant Lobes. UHECRs accelerated during the period of re-energization are more likely to contribute to an intermediate/heavy composition measured at Earth for energies above ~ 10 EeV.

In the next section, the confinement of UHECRs within the Giant Lobes will be used to constrain the episodes of activity that could be contributing to the UHECRs currently measured at Earth.

3 WHEN WERE THE UHECRS OF THE CENTAURUS EXCESS GENERATED?

The imprisoning of particles in the Lobes will result in composition-dependent flux suppression according to the particle acceleration age. Considering a point source, the density at a position r is given by the convolution of P_J with the injection rate $Q(t)$,

$$n(r, t, E) = \int_{-\infty}^{\infty} {\rm d}\tau \; Q(\tau) P_J(r, t - \tau, E). \tag{4}$$

To constrain the episode of high activity during which particles should be accelerated in Cen A, consider that the UHECR injection starts or ceases at a time t_0. It can be modelled as Heaviside step functions, $\Theta(t - t_0)$. In these cases, the particle density is given by

$$n(r, t, E) = \int_{t_0}^{\infty} {\rm d}\tau \, P_J(r, t - \tau, E) = \int_{-\infty}^{t-t_0} {\rm d}\tau \, P_J(r, \tau, E). \tag{5}$$

The flux leaving the source can be obtained via the continuity equation, $\nabla \cdot \mathbf{j} = -\partial_t n$, which can be integrated for spherical symmetry,

$$J(R, t, E) = 4\pi R^2 j = 4\pi \int_R^{ct} {\rm d}r \; r^2 \partial_t n(r, t, E), \tag{6}$$

which represents the total flux of particles with energy E leaving the source region of radius R at time t. Using equation (5), the flux leaving the source is given by[1]

$$J(R, t, E) = 4\pi \int_R^{ct} {\rm d}r \; r^2 P_J(r, t - t_0, E). \tag{7}$$

Fig. 2 presents the flux escaping the Giant Lobes, considering that acceleration occurred for $\Delta t = 2,\ 30,\ 100$ Myr (top panel) or ceased for these periods (lower panel). A strong cutoff, resulting from the diffusion time, is observed in the flux according to the source activity age and UHECR rigidity. For UHECR injection starting recently, the lightest particles are the first to escape, imposing a lower limit on the source activity age. Only protons can escape the Giant Lobes for the current AGN activity (~ 2 Myr). Nitrogen nuclei with energies ~ 20 EeV take at least 30 Myr to escape, while the situation is more dramatic for iron nuclei, where a significant fraction of events above ~ 20 EeV can escape only for an acceleration longer than ~ 100 Myr. The conclusion is reversed if the UHECR injection stopped years ago. Heavier particles are the last to escape, imposing an upper limit on the source activity age.

The excess in the *Centaurus region* extends from high energies (> 60 EeV) down to ~ 20 EeV. In this energy range, there are indications of an intermediate composition, probably Nitrogen-like (A. Abdul Halim et al. 2023b). Composition-dependent anisotropies point to an intermediate composition as well (E. Mayotte & T. Fitoussi 2023). Based on Fig. 2, Nitrogen nuclei with energies above ~ 10 EeV require the source to have been active for the last ~ 30 Myr. For iron nuclei of ~ 20 EeV to escape the source, the injection must not cease earlier than ~ 30 Myr. Note that if UHECRs are

[1]Due to numerical instabilities, the solution is combined with a truncated Gaussian for lower energies/long times, as in R. G. Lang et al. (2020).

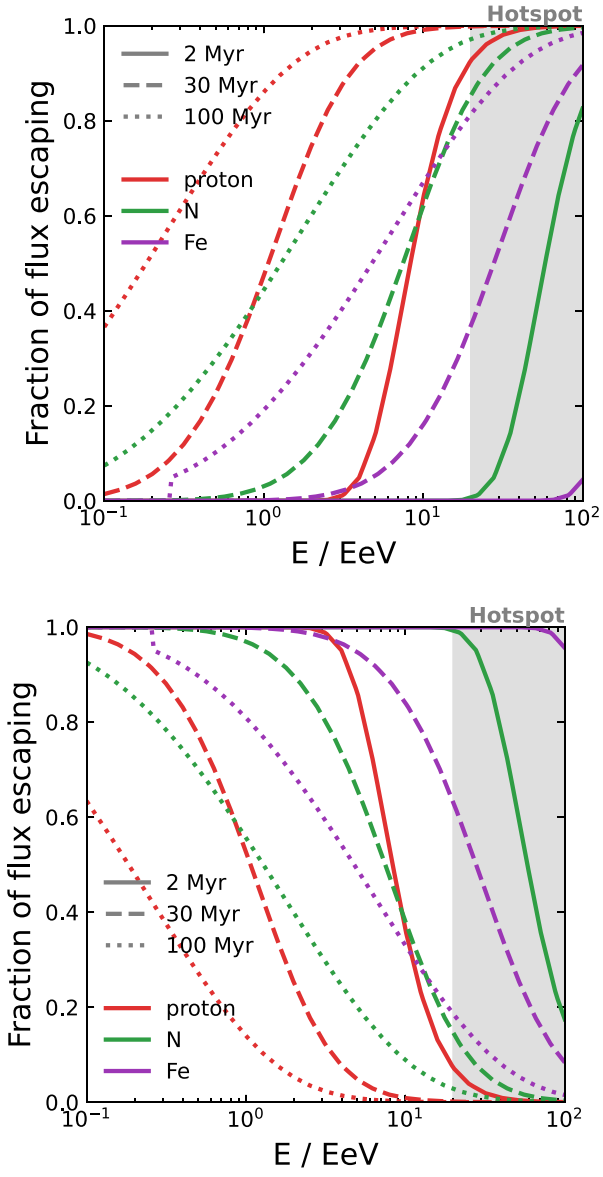

Figure 2. UHECR flux fraction escaping from the Giant Lobes for different injection scenarios. Proton, N, and Fe species are considered. Top panel: Injection starting at 2 Myr, 30 Myr, and 100 Myr. Bottom panel: Injection ceasing 2 Myr, 30 Myr, and 100 Myr ago. The energy range where the excess in the *Centaurus region* is reported (A. Abdul Halim et al. 2025b) is shown as a grey band.

not injected in the Lobes for more than $\sim$ 100 Myr, the UHECR flux above 10 EeV will be highly suppressed. These time-scales indicate that an activity for a period $\gtrsim$ 2 Myr and not ceased more than $\sim$ 30 Myr ago is necessary to accelerate UHECRs, if the central engine of Cen A is responsible for the observed UHECRs excess.

The results above suggest that a past activity $\sim$ 2–30 Myr ago may have accelerated UHECRs that are now being detected. This time-scale agrees with the re-energization time-scale of the Middle and Giant Lobes. The scenario of a recent $\lesssim$ 30 Myr activity combined with a short period of low activity is expected for Cen A. However, a long $\sim$ 50–100 Myr quiet period is highly unlike (S. G. Neff et al. 2015b).

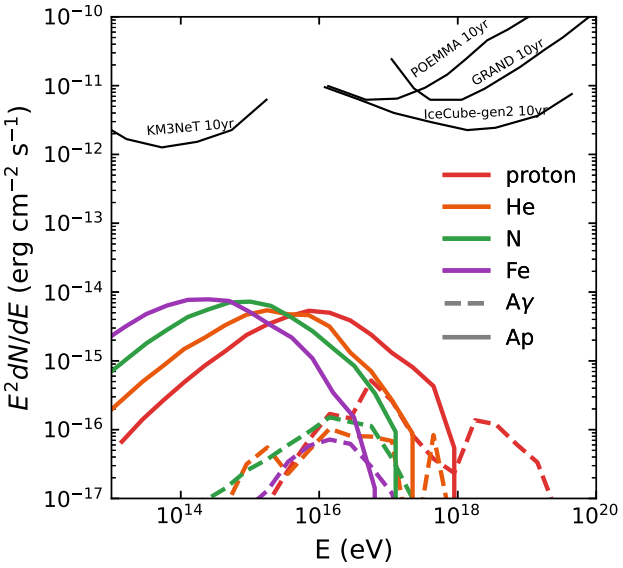

Figure 3. Upper limit for neutrino flux from photohadronic (dashed lines) and hadronic (continuous lines) interactions of UHECR within the Giant Lobes of Cen A. Different colours indicate different species. Predicted sensitivity for 10 yr observations (black lines) by KM3NeT (S. Aiello et al. 2024), POEMMA (T. M. Venters et al. 2020), GRAND (J. Álvarez-Muñiz et al. 2020), and IceCube-gen2 (R. Abbasi et al. 2021) are also showed.

3.1 Constraints from energy spectrum and composition

Based on the previous discussion, propagation through the lobes should significantly modify the energy spectrum and composition of UHECRs from Cen A. To illustrate this effect, consider a commonly adopted power-law energy spectrum with an exponential cutoff at energy $Z_j R_{\rm max}$ and spectral index s,

$$\frac{{\rm d}N}{{\rm d}E} \propto \sum_j f_j E^{-s} e^{-E/Z_j R_{\rm max}}. \quad (8)$$

Considering the power estimates for Cen A jet of $\sim 2\text{–}6 \times 10^{43}$ erg s^{-1} (S. G. Neff et al. 2015a) and equation (19) of J. H. Matthews et al. (2018b), we estimate $R_{\rm max} \sim 5\text{–}10$ EeV. For illustrative purposes, we take $s = 2$ and assume rectilinear extragalactic propagation from Cen A. As shown in Appendix A (Fig. A1), in this case, extragalactic propagation causes significant changes in the spectrum only for helium and nitrogen nuclei with energies above $\sim$ 100 EeV, where the energy spectrum is suppressed by the exponential cutoff ($E_{\rm max} = 20$ and 70 EeV, for He and N nuclei, respectively). Therefore, the extragalactic propagation will be ignored in the following analysis. This allows the effects of propagation inside the lobes to be seen more clearly.

For comparison with the energy range of events in the *Centaurus excess*, we consider an intermediate composition. As stated in the previous section, a pure nitrogen composition will be considered. Fig. 4 shows the energy spectrum escaping the lobes for the emission starting or ceasing at 2, 30, 100 Myr. For a qualitative discussion, the energy spectrum reported by the Pierre Auger Collaboration for events within the *Centaurus excess* is also presented. In this case, the high-energy events in the *Centaurus region* cannot be explained if the acceleration has ceased for $\sim$ 30 Myr under a nitrogen-like composition.

The results in Fig. 2 point to a composition strongly dependent on the age of the acceleration process. To illustrate the evolution of mass composition with energy as a function of injection time,

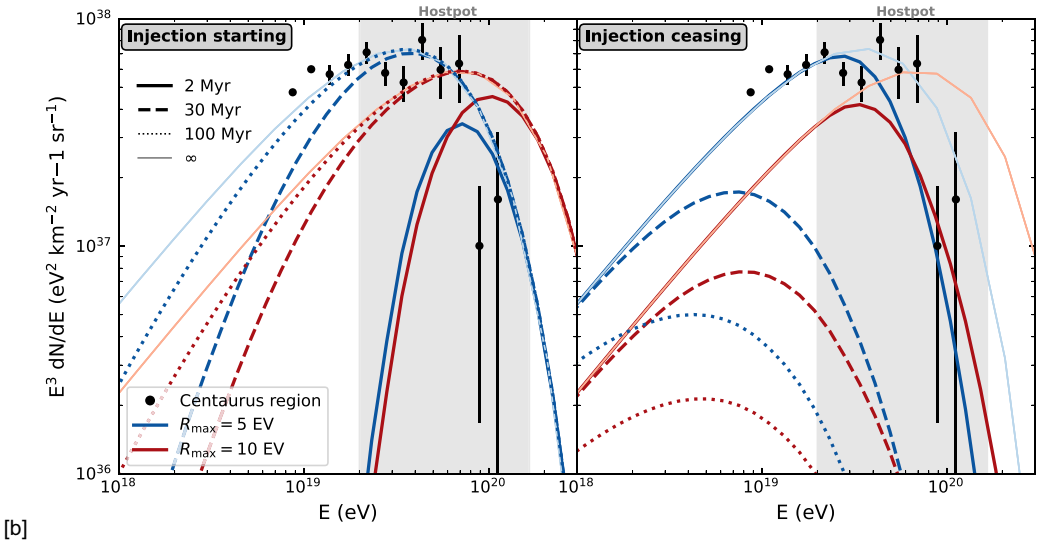

[b]

Figure 4. Energy spectrum of Nitrogen nuclei escaping the lobes of Cen A for several temporal injections. Injection starting (left) or ceasing (right) in 2, 30, and 100 Myr are shown. Two maximum rigidities, 5 (blues) and 10 EeV (reds), are considered. For comparison, the energy spectrum measured in a window 20° around Cen A is also shown (A. Abdul Halim et al. 2024). The energy spectrum of continuous infinity injection (∞) is arbitrary normalized, and corrected by the fraction of escaping flux (equation 7).

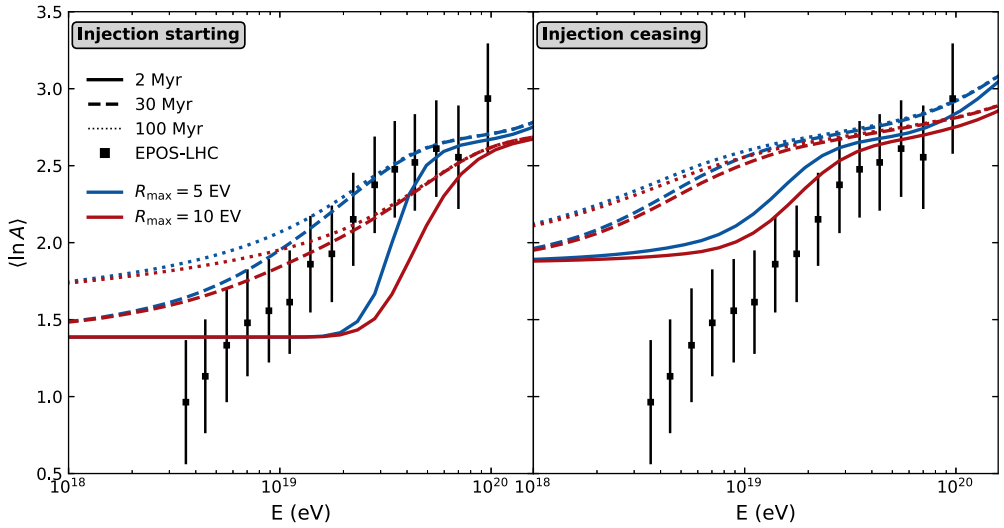

Figure 5. Evolution of the mean composition with the energy escaping the Giant Lobes for several time injections, considering a Wolf–Rayet-like composition. The mean logarithm of the composition obtained by the Pierre Auger Collaboration (A. Abdul Halim et al. 2025a) for the EPOS–LHC hadronic model is shown for comparison.

we assume a composition inspired by Wolf–Rayet stars (R.-Y. Liu et al. 2012) ($f_{\rm H} = 0$, $f_{\rm He} = 0.62$, $f_{\rm N} = 0.37$, $f_{\rm Si} = 0.01$, $f_{\rm Fe} = 0$), as suggested by A. L. Müller & A. Araudo (2025). Fig. 5 shows the evolution of $\langle \ln A \rangle$ with energy for different injection onset and cessation times for Cen A, using the two $E_{\rm max}$ values estimated above. The mean mass evolution reconstructed by the Pierre Auger Observatory (A. Abdul Halim et al. 2025a), considering the EPOS-LHC hadronic model, is also shown. In the absence of energy losses, $\langle \ln A \rangle$ is independent of the assumed spectral index s. If the source stopped the injection for a period $\gtrsim$ 2 Myr, the composition measured on Earth would be mainly heavy, in disagreement with the data. For the composition trend to be compatible with the data, it is necessary that an injection starting less than 100 Myr, with better agreement for time-scales $\lesssim$ 30 Myr. This result is consistent with our previous discussion about the time-scales for particle acceleration in Cen A.

3.2 Upper limit for neutrino emission from UHECR

Although rare, interactions within the lobes can produce secondary neutrinos and γ rays, and have been addressed by several authors (see C. a. Oliveira & V. Souza 2025 for a review). The detailed calculations performed here allow us to calculate upper limits on the neutrino flux from interactions of UHECR with the Cosmic Microwave Background, the Extragalactic Background Light (R. C. Gilmore et al. 2012), and hadronic interactions inside the Giant Lobes. The flux was computed via Monte Carlo propagations using `CRPropa` 3.2 (R. Alves Batista et al. 2022). Proton–proton interactions were

computed with the plugin of J. Dörner et al. (2025), assuming an ambient medium of HI gas. For UHECR nuclei of mass A, the neutrino flux was estimated by rescaling the proton flux by $A^{3/4}$ and shifting the neutrino energy by $1/A$ (N. Fraija et al. 2018). We propagated protons with energies between 0.1 and 1000 EeV up to the distances in Fig. 1, effectively mimicking proton, He, N, and Fe nuclei. A total of 10^4 primaries were simulated per energy bin, with 80 logarithmically spaced bins across the energy range. For simplicity, the injection spectrum was taken as $E^{-2}\exp(-E/20\ \mathrm{EeV})$. To establish upper limits, we normalized to the energy spectrum to the total UHECR spectrum measured by the Pierre Auger Observatory (P. Abreu et al. 2021), assume the injection reached steady state, and adopt an ambient gas density of 10^{-4} cm^{-3}.

Fig. 3 shows the resulting neutrino flux. The flux of photohadronic neutrinos agrees with the estimate of R. Mbarek, D. Caprioli & K. Murase (2025), reaching $\sim 10^{-16}$ erg cm^{-2} s^{-1}. Neutrinos from hadronic interactions are likely to dominate the spectra reaching $\sim 10^{-14}$ erg cm^{-2} s^{-1}. However, note that the assumed ambient gas density is an upper limit. More realistic values of $\sim 10^{-5}$ cm^{-3} (B. McKinley et al. 2022) must reduce the hadronic neutrino flux by a factor of ~ 10. Densities as lower as 10^{-8} cm^{-3} have also been proposed (S. Wykes et al. 2013). In all cases, the predicted flux remains below the detection threshold of future experiments. Unlike neutrinos, high-energy γ-rays have been detected from the lobes of Cen A, and a hadronic origin cannot be ruled out (Sun, Xiao-na et al. 2016).

4 CONCLUSION

In this paper, we place stringent constraints on the time window during which the acceleration of ultra-high-energy cosmic rays (UHECRs), currently observed at Earth and potentially originating from Cen A, must have occurred. Based on the generalized relativistic propagator of R. Aloisio et al. (2009), we developed a general expression for the escape of UHECRs from magnetized regions. By comparing the energy dependency of the *Centaurus excess*, we obtained that UHECR acceleration in Cen A must have happened $\sim$ 2–30 Myr ago. Acceleration during the recent ($\sim$ 2 Myr) reactivation of the AGN that produced the current jet and Inner Lobes cannot explain the energy spectrum measured in the *Centaurus excess* region when an intermediate, nitrogen-like composition is assumed. Likewise, injection in a distant past activity, $\gtrsim$ 100 Myr, is constrained by energetic and composition arguments. This indicates that the formation of the Giant Lobes ($\sim$ Gyr) cannot account for the detected high-energy events.

If Cen A were the dominant source of ultra-high-energy cosmic rays (UHECRs) at extreme energies, injecting primarily light or intermediate-mass nuclei (P. L. Biermann & V. Souza 2012; S. Mollerach & E. Roulet 2024), one would expect a detectable clustering of events at $\gtrsim$ 100 EeV in its direction. However, the escape time for UHECRs from the Giant Lobes at these energies is ballistic, taking $\sim$ 0.6 Myr (see Fig. A1). A temporary reduction in the source's activity over this time-scale would be sufficient to suppress the ongoing detection of such extreme events from Cen A. In this scenario, only heavier nuclei – potentially confined within the lobes for extended periods ($\sim$ 2 Myr) – could escape. These nuclei experience greater deflections in Galactic and extragalactic magnetic fields due to their higher charge, which can lead to the observed isotropy at the highest energies. Consequently, the lack of a significant excess of events at $\gtrsim$ 100 EeV in the direction of Cen A can be explained by a relatively short ($\sim$ 0.6–2 Myr) quiescent phase – consistent with the episodic nature of Cen A's activity (S. G. Neff et al. 2015b) – or by limitations in its ability to accelerate particles beyond this energy. In both cases, the particles escaping the lobes at the highest energies are expected to be predominantly heavy nuclei.

In this work, we assume that Cen A is the source of the excess of events in the *Centaurus region*. For this purpose, we adopt the conservative assumption that extragalactic and Galactic magnetic fields are not strong enough to cause more than intermediate-scale deflections. The potential impact of both structured and turbulent magnetic fields on the arrival directions and energy spectrum of UHECRs from Cen A has been addressed in previous studies (C. a. Oliveira & V. de Souza 2022, 2023; S. Mollerach & E. Roulet 2024; R. Mbarek & D. Caprioli 2025). As we have shown in a previous work (C. a. Oliveira & V. de Souza 2022), heavy iron-like species can suffer strong deflections due to the EGMF and GMF. In particular, S. Mollerach & E. Roulet (2024) showed that Cen A could be the dominant contributor to the total UHECR spectrum when both extragalactic magnetic fields and the finite source lifetime are considered. The maximum rigidity obtained in their combined fit ($\sim$ 5–10 EeV) is compatible with the values adopted in this work. Although only diffusive scattering is considered in S. Mollerach & E. Roulet (2024), additional intermediate-scale excesses in the arrival directions could arise from deflections in the magnetic structures of Starburst Galaxies (A. R. Bell & J. H. Matthews 2022) and in the *Council of Giants* (A. M. Taylor, J. H. Matthews & A. R. Bell 2023). A scenario in which Cen A is the only dominant source is consistent with a small variance in maximum rigidity required to reproduce the UHECR spectrum and composition, as reported by D. Ehlert, F. Oikonomou & M. Unger (2023).

The quantitative framework developed in this work opens the venue for future studies considering individual properties of other local radio galaxies. In addition to Cen A, other radio galaxies have been explored as potential sources of UHECRs (J. H. Matthews et al. 2018a; B. Eichmann, M. Kachelrieß & F. Oikonomou 2022; C. a. Oliveira & V. de Souza 2022; C. a. Oliveira, R. G. Lang & P. Batista 2025). As argued by J. H. Matthews et al. (2018b), nearby powerful radio galaxies are rare, making it challenging to account for the observed UHECR luminosity density based solely on their current jet power. The authors also point out that the reservoirs of UHECRs could mitigate this issue if the jets undergo periods of enhanced activity. K. Ehlert et al. (2022) demonstrated that, in general, AGNs can be highly intermittent depending on the accretion mode, while the inferred cavity luminosity is dependent on the average jet power. Taken together with our results, this indicates that the AGN activity must be integrated over time-scales of many Myr. This not only alleviates the luminosity density constraint but also favours a heavier composition for UHECR, which takes longer to escape.

In this work, we have shown that the current activity of Cen A is unlikely to produce the events detected in the *Centaurus excess*. The observed energy and composition of the UHECR excess suggest acceleration time-scales on the order of $\sim$ 2–30 Myr, aligning well with the recent re-energization episodes of the Middle and Giant Lobes of Cen A. This temporal consistency strongly supports the hypothesis that these structures are responsible for the observed excess. Given the established evidence of past activity in Cen A, attributing the *Centaurus excess* to this source is both plausible and well supported by current observational data.

ACKNOWLEDGEMENTS

CdO thanks Henrique Malavazzi and Leonardo Paulo Maia for useful discussions. This study was financed, in part, by the São Paulo Research Foundation (FAPESP), Brasil. Process Number 2025/03325-5, 2021/01089-1, 2020/15453-4, and 2019/10151-2.

VdS is supported by Conselho Nacional de Desenvolvimento Científico e Tecnológico (CNPq) – process 308837/2023-1.The authors acknowledge the National Laboratory for Scientific Computing (LNCC/MCTI, Brazil) for providing HPC resources of the SDumont supercomputer, which have contributed to the research results reported within this paper. URL: http://sdumont.lncc.br

DATA AVAILABILITY

The data produced as part of this work are available from the authors on reasonable request.

REFERENCES

Abbasi R., et al., 2021, PoS, ICRC2021, 1183
Abdul Halim A. et al., 2023a, PoS, ICRC2023, 252
Abdul Halim A. et al., 2023b, PoS, ICRC2023, 438
Abdul Halim A. et al., 2024, J. Cosmol. Astropart. Phys., 2024, 022
Abdul Halim A. et al., 2025a, Phys. Rev. D, 111, 022003
Abdul Halim A. et al., 2025b, ApJ, 984, 123
Abreu P., et al., 2021, Euro. Phys. J. C, 81, 966
Aharonian F. A., 2002, MNRAS, 332, 215
Aiello S., et al., 2024, Astropart. Phys., 162, 102990
Aloisio R., Berezinsky V., Gazizov A., 2009, ApJ, 693, 1275
Álvarez-Muñiz J. et al., 2020, Sci. China Phys. Mech. Astron., 63, 219501
Alves Batista R. et al., 2022, J. Cosmol. Astropart. Phys., 2022, 035
Batista R. A. et al., 2016, J. Cosmol. Astropart. Phys., 2016, 038
Bell A. R., Matthews J. H., 2022, MNRAS, 511, 448
Biermann P. L., de Souza V., 2012, ApJ, 746, 72
Cronin J. W., 1999, Rev. Mod. Phys., 71, S165
Croston J. H. et al., 2009, MNRAS, 395, 1999
Dörner J., Morejon L., Kampert K.-H., Becker Tjus J., 2025, J. Cosmology Astropart. Phys., 2025, 043
Ehlert D., Oikonomou F., Unger M., 2023, Phys. Rev. D, 107, 103045
Ehlert K., Weinberger R., Pfrommer C., Pakmor R., Springel V., 2022, MNRAS, 518, 4622
Eichmann B., Kachelrieß M., Oikonomou F., 2022, J. Cosmol. Astropart. Phys., 2022, 006
Eilek J. A., 2014, New J. Phys., 16, 045001
Fraija N., Aguilar-Ruiz E., Galván-Gámez A., Marinelli A., de Diego J. A., 2018, MNRAS, 481, 4461
Gilmore R. C., Somerville R. S., Primack J. R., Domínguez A., 2012, MNRAS, 422, 3189
Greisen K., 1966, Phys. Rev. Lett., 16, 748
Harari D., Mollerach S., Roulet E., Sánchez F., 2002, J. High Energy Phys., 2002, 045
Harari D., Mollerach S., Roulet E., 2014, Phys. Rev. D, 89, 123001
Hardcastle M. J., Cheung C. C., Feain I. J., Stawarz L., 2009, MNRAS, 393, 1041
Harris G. L., Rejkuba M., Harris W. E., 2010, Publ. Astron. Soc. Aust., 27, 457
He H.-N., et al., 2024, (arXiv:2412.11966),
Israel F., 1998, Astron. Astrophys. Rev., 8, 237
Lang R. G., Taylor A. M., Ahlers M., de Souza V., 2020, Phys. Rev. D, 102, 063012
Linsley J., 1963, Phys. Rev. Lett., 10, 146
Liu R.-Y., Wang X.-Y., Wang W., Taylor A. M., 2012, ApJ, 755, 139
Müller A. L., Araudo A. L., 2025, in Proceedings of 7th International Symposium on Ultra High Energy Cosmic Rays - PoS(UHECR2024), p. 105
Matthews J. H., Taylor A. M., 2021, MNRAS, 503, 5948
Matthews J. H., Bell A. R., Blundell K. M., Araudo A. T., 2018a, MNRAS, 479, L76
Matthews J. H., Bell A. R., Blundell K. M., Araudo A. T., 2018b, MNRAS, 482, 4303
Mayotte E., Fitoussi T., 2023, EPJ Web Conf., 283, 03003
Mbarek R., Caprioli D., 2025, Astropart. Phys., 172, 103148
Mbarek R., Caprioli D., Murase K., 2025, Phys. Rev. D, 111, 023024
McKinley B. et al., 2022, Nat. Astron., 6, 109
Mollerach S., Roulet E., 2024, Phys. Rev. D, 110, 063030
Neff S. G., Eilek J. A., Owen F. N., 2015a, ApJ, 802, 87
Neff S. G., Eilek J. A., Owen F. N., 2015b, ApJ, 802, 88
O'Sullivan S., Reville B., Taylor A. M., 2009, MNRAS, 400, 248
de Oliveira C. a., de Souza V., 2022, ApJ, 925, 42
de Oliveira C. a., de Souza V., 2023, J. Cosmol. Astropart. Phys., 2023, 058
de Oliveira C. a., de Souza V., 2025, Int. J. Mod. Phys. A, p. 2530016 40
de Oliveira C. a., Lang R. G., Batista P., 2025, ApJ, 981, 123
Rieger F. M., 2022, Universe, 8, 607
Romero G. E., Combi J. A., Perez Bergliaffa S. E., Anchordoqui L. A., 1996, Astropart. Phys., 5, 279
Stefan I. I. et al., 2013, MNRAS, 432, 1285
Sun X.N., Yang, Rui-zhi R. Z., Mckinley B., Aharonian F., 2016, A&A, 595, A29
Taylor A. M., Matthews J. H., Bell A. R., 2023, MNRAS, 524, 631
The H.E.S.S. Collaboration, 2020, Nature, 582, 356
Venters T. M., Reno M. H., Krizmanic J. F., Anchordoqui L. A., Guépin C., Olinto A. V., 2020, Phys. Rev. D, 102, 123013
Wykes S. et al., 2013, A&A, 558, A19
Wykes S. et al., 2014, MNRAS, 442, 2867
Wykes S., Hardcastle M. J., Croston J. H., 2015, MNRAS, 454, 3277
Zatsepin G. T., Kuzmin V. A., 1966, JETP Lett., 4, 78

APPENDIX A: ENERGY LOSSES INSIDE THE LOBES

During propagation, the energy spectrum can be modified by hadronic and photohadronic interactions. Modulations of the spectrum will be relevant if the interaction and escape time-scales are comparable, $\tau_{\rm int} \lesssim \tau_{\rm esc}$. We consider photohadronic interactions with the cosmic microwave background and extragalactic background light (R. C. Gilmore et al. 2012) for redshift $z = 0$, obtained using the `CRPropa` code (R. A. Batista et al. 2016).

Hadronic (proton–proton or nucleus–proton) interactions can occur with the thermal material of the lobes of density n_{th}. Since the proton–proton cross section is weakly dependent on energy, we follow previous works writing $\tau_{\rm pp} \approx 1.7 \times 10^6 n_{-4}^{-1}$ Myr, where $n_{th} = 10^{-4} n_{-4}$ cm^{-3} (F. A. Aharonian 2002; M. J. Hardcastle et al. 2009; N. Fraija et al. 2018). Taking $n_{-4} \sim 0.1$–1 (B. McKinley et al. 2022) results in $\tau_{\rm pp} \sim 10^6$–10^7 Myr. For a nucleus of mass A, the cross section increases by $A^{3/4}$, leading to a decrease by a factor ~ 20 for ^{56}Fe in the time-scale.

Fig. A1 presents $\tau_{\rm esc}$, $\tau_{\rm int}$, and $\tau_{\rm adv}$ for different species (proton, ^{4}He, ^{14}N, ^{56}Fe), compared with the ages of different structures in Cen A (left panel). To determine the importance of interactions over the energy spectrum, the ratio $\tau_{\rm esc}/\tau_{\rm int}$ is also shown (right panel). In general, $\tau_{\rm esc}/\tau_{\rm int} \ll 1$, indicating that modulations of the energy spectrum by interactions inside the Giant Lobes are unlike.

Hadronic interactions take place on time-scales much longer than needed for escape, and are not shown. UHECR of high energy realize rectilinear trajectories, and escape the lobes after ~ 0.6 Myr. However, diffusion starts to be important for lower energies ($\lesssim 10$ EeV for protons and $\lesssim 100$ EeV for Nitrogen), causing a significant delay in the escape time. In general, advection is only important below ~ 1 EeV and can be neglected for our purposes.

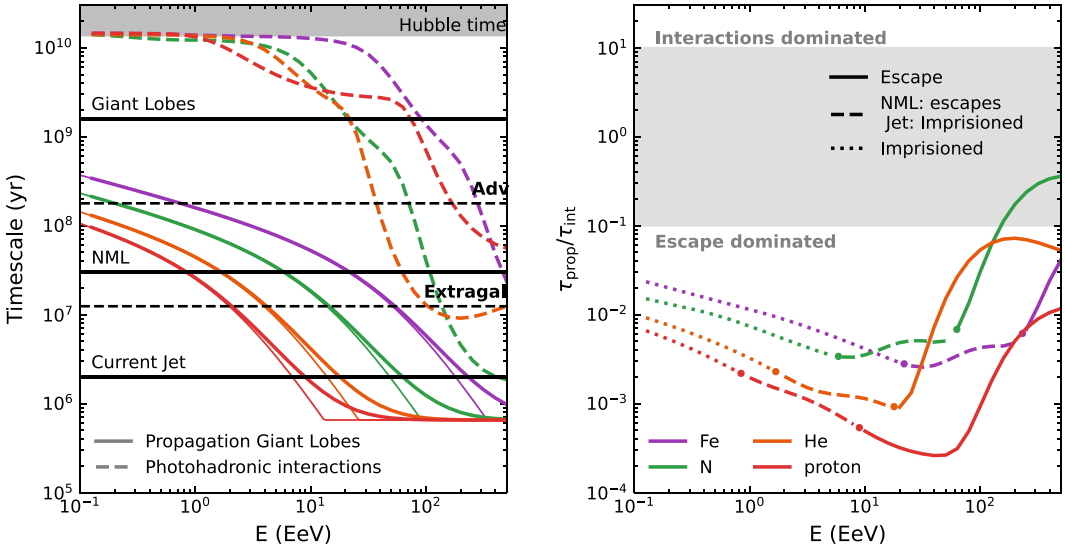

Figure A1. Time-scales for Cen A. Left panel: Time-scales for propagation of different UHECR species (continuous coloured line) in the Giant Lobes are shown together with time-scales for different structures in Cen A (continuous black lines). Interaction time-scales for the CMB and EBL are shown in dashed lines. Black dashed lines are estimations for the extragalactic time interval necessary UHECR to reach Earth, considering a rectilinear trajectory (Extragal), and the advection time-scale inside the lobes (Adv). Together with the propagation time, thin continuous lines represent the propagation time-scale for rectilinear and diffusive regimes. Right panel: Ratio between propagation and interaction time-scales for different UHECR species. Continuous lines indicate the fraction of UHECR expected to escape from the Giant Lobes, both if generated in the re-energization (NML, $\sim$ 30 Myr) or the current jet time-scale ($\sim$ 2 Myr). Dashed lines indicate escape if accelerated on Middle Lobe re-energization, but not if injected during the current activity. Dotted lines indicate the fraction that remains imprisoned. The grey band represents the transition between a regime escape- or interaction-dominated.

This paper has been typeset from a TEX/LATEX file prepared by the author.